Broadband optical absorbance spectroscopy using a whispering gallery mode microsphere resonator

Sarah L. Westcott,[1] Jiangquan Zhang,[1] Robert K. Shelton,[1] Nellie M. K. Bruce,[1] Sachin Gupta,[1] Steven L. Keen,[1] Jeremy W. Tillman,[1] Lara B. Wald,[1] Brian N. Strecker,[1] A. T. Rosenberger,[2] Roy R. Davidson,[3] Wei Chen,[3] Kevin G. Donovan,[3] and John V. Hryniewicz[3]

[1]*ICx Nomadics, 1024 S. Innovation Way, Stillwater, Oklahoma 74074, USA*
[2]*Department of Physics, Oklahoma State University, Stillwater, Oklahoma 74078, USA*
[3]*PLC Division, Infinera, 9020 Junction Drive, Annapolis Junction, Maryland 20701, USA*

(Received 21 August 2007; accepted 18 February 2008; published online 13 March 2008)

We demonstrate the ability to excite and monitor many whispering gallery modes (WGMs) of a microsphere resonator simultaneously in order to make broadband optical absorbance measurements. The 340 μm diameter microsphere is placed in a microfluidic channel. A hemispherical prism is used for coupling the WGMs into and out of the microsphere. The flat surface of the prism seals the microfluidic channel. The slight nonsphericity in the microsphere results in coupling to precessed modes whose emission is spatially separated from the reflected excitation light. The evanescent fields of the light trapped in WGMs interact with the surrounding environment. The change in transmission observed in the precessed modes is used to determine the absorbance of the surrounding environment. In contrast to our broadband optical absorbance measurements, previous WGM sensors have used only a single narrow mode to measure properties such as refractive index. With the microfluidic cell, we have measured the absorbance of solutions of dyes (lissamine green B, sunset yellow, orange G, and methylene blue), aromatic molecules (benzylamine and benzoic acid), and biological molecules (tryptophan, phenylalanine, tyrosine, and *o*-phospho-L-tyrosine) at visible and ultraviolet wavelengths. The microsphere surface was reacted with organosilane molecules to attach octadecyl groups, amino groups, and fluorogroups to the surface. Both electrostatic and hydrophobic interactions were observed between the analytes and the microsphere surface, as indicated by changes in the measured effective pathlength with different organosilanes. For a given analyte and coated microsphere, the pathlength measurement was repeatable within a few percent. Methylene blue dye had a very strong interaction with the surface and pathlengths of several centimeters were measured. Choosing an appropriate surface coating to interact with a specific analyte should result in the highest sensitivity detection. © *2008 American Institute of Physics.* [DOI: 10.1063/1.2894307]

I. INTRODUCTION

From the early 20th century, absorbance-spectroscopy-based measurements have dominated chemical analysis. Thousands of colorimetric and spectrometric assays have been employed in almost every area from medicine to process control. Even today, colorimetric and spectrometric assays have proved particularly useful in biochemical analysis and are routinely used in the clinical laboratories of modern hospitals for blood and urine analyses.[1] Ultraviolet (UV) absorbance is the most common detection method used for HPLC.[2]

Meanwhile, breakthrough interdisciplinary developments have resulted in a plethora of companies developing assays, diagnostics, instruments, and devices based on microfluidics technology.[3,4] The advantages of making measurements of microvolume samples are significant. These include the dramatic reduction in analysis time achievable with on-chip separations and the ability to perform large numbers of parallel analyses using microarrays. However, the huge library of existing absorbance-based spectroscopic methods is being left behind because these tests depend on pathlength to obtain sufficient sensitivity and also require two optically smooth surfaces. Fluorescence detection is used for many microtechnology applications, but challenges include the need to incorporate fluorophore tagged target analytes and the fact that fluorescent tags are not available for many important classes of target analytes.

We demonstrate here the ability to make broadband absorbance measurements in microfluidic channels using microspheres, which are small glass spheres with diameters between 1 and 1000 μm that are capable of supporting whispering gallery modes (WGMs).[5–7] A glass sphere with a higher refractive index than the surrounding environment can trap light by total internal reflection from its surface. Light propagating inside the sphere is then spatially constrained to travel repeatedly along the perimeter of an equatorial plane. The quality factor or Q is usually defined as 2π times the ratio of energy stored to energy dissipated in the microsphere. Loss mechanisms include absorption, scattering from the surface, and light coupled out. Microspheres with a

higher Q circulate and store light more efficiently. In addition to microspheres, other structures are also capable of WGM resonance,[8] including disks, cylinders, tori, ring resonators, and thin walled capillaries.[9]

Although light is tightly confined in this WGM resonance, a small amount of energy extends outside the surface of the sphere in the form of an evanescent field. For a microsphere resonator, the evanescent decay length is approximately

$$\frac{\lambda}{2\pi\sqrt{n_s^2 - n_o^2}}, \tag{1}$$

where λ is the wavelength, n_s is the refractive index of the microsphere, and n_o is the refractive index of the surrounding medium. At 633 nm, for a fused silica microsphere (n_s=1.457) in water (n_s=1.333), the decay length is ~27% of the wavelength or 170 nm. For the microsphere resonator, the interaction length between the light and the sample is the perimeter of the sphere, which is about 1 mm, and the interaction only occurs for the evanescent part of the WGMs, which is on the order of 1% of the total energy. However, the WGMs circulate around the microsphere hundreds of thousands of times before being coupled out of the resonator. This recirculation greatly increases the effective interaction pathlength between the light and the sample. As a result, the microsphere WGM resonator has the potential for higher sensitivity compared to a conventional absorbance spectrometer.

Coupling into and out of microspheres is accomplished by overlapping the evanescent field of the microsphere with the evanescent field from tapered fibers,[10–12] angle-polished fibers, waveguides,[13] or prisms.[14] We have found prism coupling to be especially suited for microspheres embedded in microfluidic chips because the prism can also form one of the surfaces of the microfluidic channel. The coupling coefficient can be adjusted by altering the prism-resonator spacing.

Wavelengths (and angles) that result in constructive overlap of electric fields build up in a WGM. Since the light resonating inside the sphere is thus phase matched with the input energy, the intensity of the WGM may accumulate from the input source, enhancing both the internal and evanescent fields.[15,16] Most microsphere applications use single wavelength, continuous wave lasers and highly precise, narrowband detectors to monitor or select a single resonant mode with the highest possible Q factor.[17] This is done in order to have narrow resonance linewidths, large optical fields, and long decay times. These applications[8,18] include optical communications filters, cavity quantum electrodynamics, microlasers, and refractive index sensors.[9,19,20]

For an eccentric microsphere which deviates from a perfect sphere, there are nondegenerate, higher order modes that exist off the resonator's equatorial plane. This leads to some of the trapped light being coupled into a precessed mode. This light couples out of the microsphere at a different angle than light that simply reflects off the prism-coupling interface or couples out from the originally excited mode. This two-lobe emission occurs for both single wavelength[21] and broadband[22] light sources.

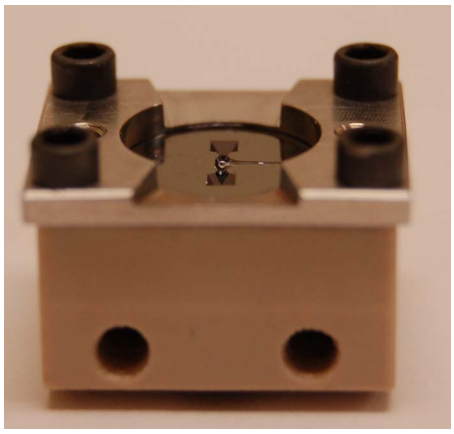

FIG. 1. (Color online) The V-groove microfluidic channel runs from top to bottom in this image. The square holes at the top and bottom are the fluidic openings. The microsphere can be seen at the center of the main channel. The fiber stem from the microsphere is soldered into the channel to the right.

Although only discrete WGMs are permitted, the wavelength separation between modes is small compared to the resolution required for an absorbance measurement. Therefore, many modes can be simultaneously excited and measured using a broadband light source and a detector that averages over many modes—as for the absorbance spectroscopy measurements presented here.

II. DESIGN

Microfluidic channels using a V-groove shape were fabricated on small chips by etching silicon wafers (PLC Division, Infinera, Annapolis Junction, MD). A region on each end of the channel was etched entirely through the substrate to form the fluidic openings. Microspheres of 340 μm diameter were made by heating the end of an optical fiber with a CO_2 laser. When the tip melted, surface tension forced the molten silica into a near-perfect microsphere.[5] The fiber was spun on axis to prevent drooping of the molten silica sphere. A short length of the optical fiber was kept attached to the microsphere and was used to secure the microsphere in the fluidic channel using glass solder. Figure 1 shows the microfluidic chip with a microsphere soldered in place. The chip is sitting on top of a holder with fluidic connections. After the fiber stem was soldered in place, the microfluidic chip (including the microsphere) was piranha etched (35 ml H_2SO_4 and 15 ml, 30%–35% aqueous H_2O_2 for 30 min), rinsed with water and then ethanol, and dried in a 120 °C oven for at least 1 h. Many of the microspheres were treated with organosilanes to provide a surface coating ranging from hydrophobic to polar. Silanized or uncoated microspheres were then ready for mounting of a prism.

For measurements with visible dyes, the following silanes were used:

(1) Octadecylsilane (ODS) treatment: Chloro(dimethyl)octadecylsilane was liquefied by heating (about 30 °C) and dissolved in hexanes to a concentration of 5 ml/l under a nitrogen atmosphere. The microfluidic chip (including microsphere) was placed in this solution for

10 min, rinsed with hexanes, and allowed to dry in the nitrogen atmosphere.

(2) Aminosilane treatment: Microfluidic chips were placed in a 5% solution of 3-aminopropyltriethoxysilane (APTES) in 95% ethanol and 5% water for 30 min, then subsequently rinsed with ethanol, and dried in a 120 °C oven.

(3) Fluorosilane treatment: $1H,1H,2H,2H$ perfluorodecyltriethoxysilane (PFDTES) was dissolved to a 10% concentration in a solution of 95% ethanol, 5% water, and 10 mM acetic acid. The microfluidic chip was placed in this solution for 30 min, rinsed with ethanol, and dried in a 120 °C oven.

For measurements with benzylamine and benzoic acid, we used the following silanes:

(1) APTES treatment: Microfluidic chips were placed in a 5% solution of APTES in toluene and allowed to react for 1 h followed by rinses with toluene and ethanol, and drying in a 120 °C oven.

(2) 3-aminopropylmethyldiethoxysilane (APMdES) treatment: Same concentration and times as APTES.

(3) 3-aminopropyldimethylethoxysilane (APdMES) treatment: Same concentration and times as APTES.

These silanes have three, two, and one reactive alkoxy groups each and will cross-link with the silica surface of the microspheres to different extents. The different aminosilanes were tested to determine whether the concentration of amine groups on the microsphere surface affected the pathlength.[23]

During the silanization reaction, –Cl, $–OCH_3$, and $–OCH_2CH_3$ groups are converted to –OH groups. These –OH groups react with –OH groups on the surface of the silica microsphere.[24] The benefit of using a molecule with only one active group (like the ODS) is that only a monolayer can form. For the molecules with three reactive groups, such as the aminosilane APTES and fluorosilane PFDTES, the silane molecules can bind to each other as well as the microsphere surface, leading to a thicker three-dimensional coating. For these trialkoxy silanes, there are generally more of the amine or fluorine groups available near the surface, but the exact thickness of the coating and density of the groups are difficult to control.

The assembly of the microchip device is shown in Fig. 2. After coating a microchip with silane, the chip was placed on a base. The fluidic connections were made to that base. A hemispherical prism was mounted on top of the chip. To seal the prism to the chip, a gasket with an opening larger than the channel was cut out of a thin polydimethylsiloxane sheet that was prepared using Dow Corning Sylgard 184. The gasket has a thickness of ~30 μm and was placed over the microchip. The prism was placed on the gasket, with the flat surface of the prism enclosing the microfluidic channel. A bar was placed over the curved surface of the prism and clamped down using screws into holes on top of the chip holder (holes visible in Fig. 1 on the left and right sides between the top screws). Prisms made of BK7 glass or sapphire were used for visible or UV wavelength measurements, respectively.

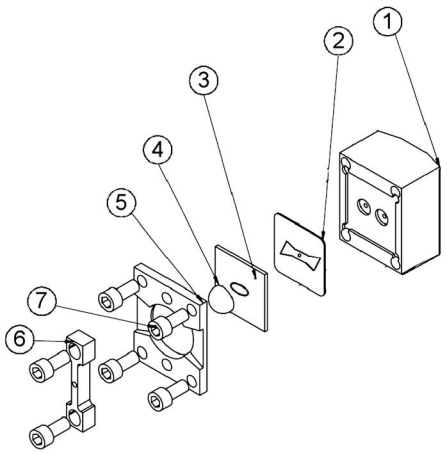

FIG. 2. The microfluidic chip (2) is placed on a base (1). A gasket (3) is held in place by a cover (5) using screws (7). The hemispherical prism (4) is placed on the chip and held in place using a bar (6) with additional screws.

Light from a white light source or, more usually, from a light emitting diode (LED) was coupled into an optical fiber and focused using a lens tube through the hemispherical prism onto the microsphere. Due to the nonspherical nature of the microsphere, the initially excited modes transfer some of their energy to precessed modes. The light is therefore coupled out at two different angles.[21] The nonprecessed light overlaps with light that is reflected from the prism/microsphere interface without coupling. The precessed light is spatially separated from the reflected light and was collected after the hemispherical prism using a lens tube and coupled into the optical fiber. This transmitted light was measured using an Ocean Optics QE65000 spectrometer (a USB2000 spectrometer was used for initial measurements).

The light that is coupled into the microsphere has an evanescent component that interacts with the environment around the surface of the microsphere (in this case, the analyte). This evanescent fraction varies for each mode of the microsphere but is on the order of 1% of the light energy in the microsphere for a fused silica microsphere of 340 μm diameter in water. However, because the Q of the microsphere can be on the order of 10^4–10^7 even in water, the light has many opportunities to interact with the environment and potentially a large effective pathlength.

Figure 3 is a schematic showing the pumps and valves used to control the flow of water, alcohol, and analyte-containing solutions through the microfluidic chip and past the microsphere. A six-port valve (Cheminert C22-3186EH) controls whether the pump refills from a de-ionized (DI) water supply or infuses to deliver water through the system to the microsphere platform. During refill, DI water (or buffer solution) is degassed using a UniFlows Degasys Ultimate DU4010 degasser and used to fill a 50 ml syringe mounted on a Harvard Apparatus PHD 2000 syringe pump. During infusion, the water from the syringe is pumped a second time through the degasser to remove any air bubbles. A ten-port valve (Cheminert C22Z-3180EH) with two positions is used to direct the water through one of two sample loops. In the position shown, the water entering at port 4 is connected by the valve to port 3. Ports 3 and 10 are connected by a loop of

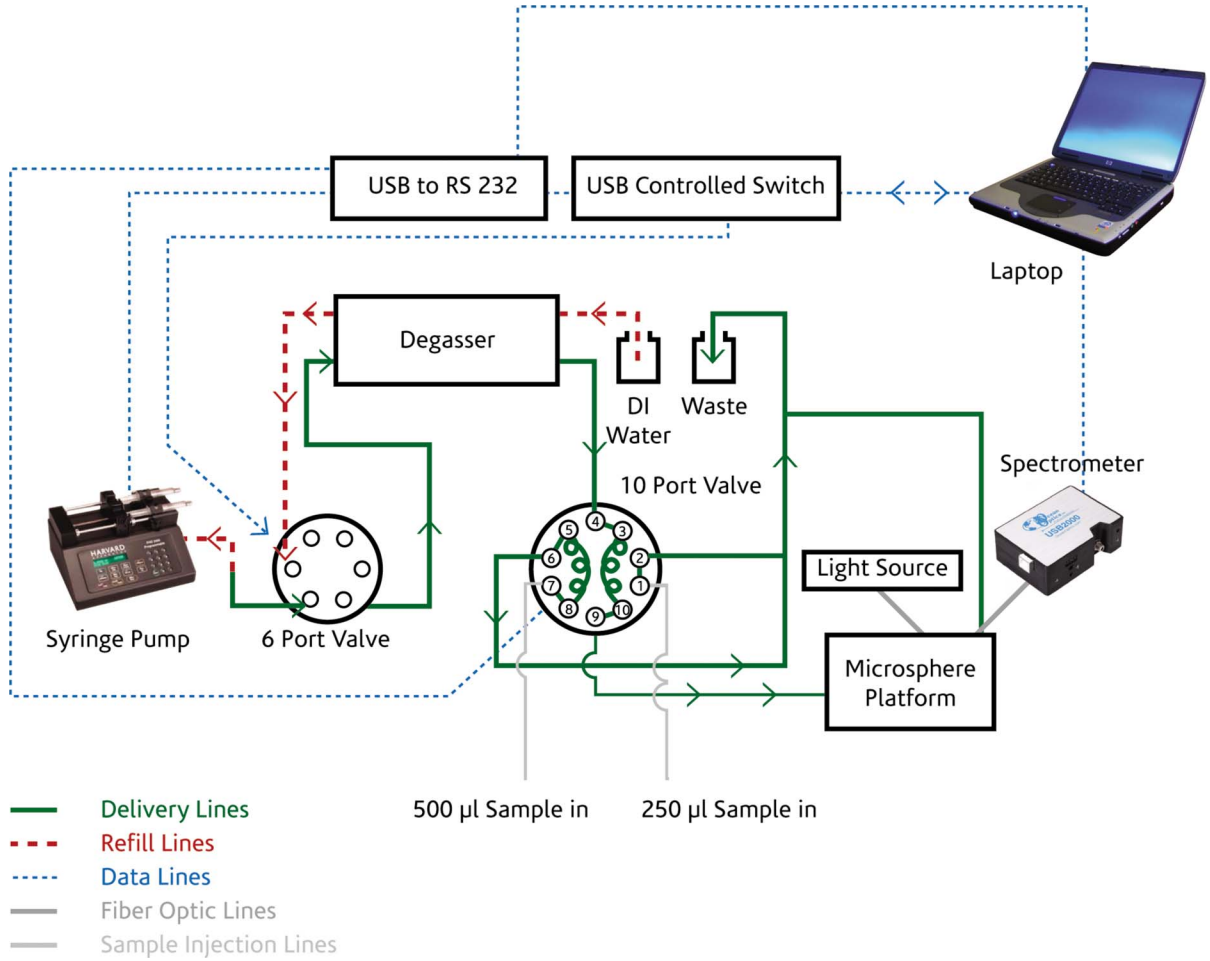

FIG. 3. (Color online) The experimental setup used to measure the optical transmission through the microsphere and control the flow of water and analyte-containing solutions past the microsphere.

tubing with a volume of 250 μl. Port 10 is connected by the valve to port 9, which directs the water to the microfluidic platform, past the microsphere, and to the waste. Meanwhile, the analyte solution can be injected through port 7 to fill a sample loop with a volume of 500 μl. Any excess is directed through port 6 to the waste. When the analyte solution is desired, the valve positions are switched such that port 4 is connected to port 5 and port 8 is connected to port 9. Then the water from the pump forces the analyte solution ahead of it through the 500 μl sample loop to the microsphere platform.

The fluidic system was controlled by custom software which allowed valve switches either at regular time intervals or on demand. The software also received the output from the spectrometer and plotted the transmitted light as a function of time.

A. Chemicals

Chemicals purchased from Sigma-Aldrich included chloro(dimethyl)octadecylsilane, APTES, PFDTES, acetic acid, lissamine green B (LGB), sunset yellow (SY) FCF, orange G (OG), methylene blue (MB), benzoic acid, benzylamine, L-phenylalanine, L-tryptophan, L-tyrosine, *o*-phospho-L-tyrosine, sodium citrate, citric acid, 4-morpholine-ethanesulfonic (MES) acid hydrate, and potassium phosphate monobasic. Sodium hydroxide was purchased from VWR. Hydrochloric acid, toluene, and ethanol were purchased from Pharmco-Aaper. Chemicals purchased from Gelest included APMdES and APdMES. All chemicals were used as received without further purification.

In general, water with a resistance of 18.2 MΩ from a DI water system was used to make solutions (Barnstead E-Pure). For the fluidic system, 99.9% Chromasolv Plus HPLC grade water and isopropanol from Sigma-Aldrich were used. 17 mM sodium citrate/citric acid buffer solutions at *p*H 5 were prepared by adding 0.26 g citric acid and 0.63 g sodium citrate to 200 ml water. 17 mM phosphate buffer solutions at *p*H 7 were prepared by adding 1.15 g potassium phosphate monobasic and 0.13 g sodium hydroxide to 500 ml water. For *p*H 9 buffer solutions, 0.33 g sodium hydroxide was used instead. 10 mM MES buffer solutions were prepared by dissolving MES acid in water and adding sodium hydroxide to raise the *p*H to 5.5.

III. ABSORBANCE MEASUREMENTS

A. Theory

The absorbance A through a cuvette is given by Beer's law:

$$A = \log(I_o/I) = C\varepsilon L/2.3, \tag{2}$$

where I_o is the light transmitted without the analyte, I is the light transmitted with the analyte present, C is the concentration of the analyte, ε is the molar extinction coefficient of the analyte,[25] and L is the pathlength through the cuvette.

The amount of light transmitted through the microsphere depends on both losses of the microsphere system (coupling coefficients to and from the microsphere as well as absorbance and scattering losses of the microsphere silica material and the surface of the microsphere) as well as the loss due to absorbance of the analyte. This results in a different expression for the transmission:[26]

$$\frac{T_a}{T_o} = \frac{1}{(1 + 0.5C\varepsilon L_{\text{eff}})^2}. \tag{3}$$

T_a is the transmitted light in the presence of the analyte, T_o is the transmitted light without the analyte, and L_{eff} is the effective pathlength of the microsphere. Note that if there is only a small change in transmission, the Taylor expansions of T_a/T_o and I/I_o are identical. As defined in Eq. 12 of Ref. 26,

$$L_{\text{eff}} = \frac{2fL}{2T + \alpha_i L} = \frac{f\lambda Q}{\pi n}, \tag{4}$$

where f is the evanescent fraction of the waveguide mode, L is the microresonator circumference (round-trip length), T is the transmission of the waveguide mode for a single round-trip without the analyte, α_i is the intrinsic loss coefficient of the microsphere, λ is the wavelength of the light, Q is the microsphere quality factor, and n is the index of refraction in the microsphere.

Substituting $C\varepsilon$ from Eq. (2) into Eq. (3), we expect a proportional relationship between the $\sqrt{T_o/T_a} - 1$ and the absorbance A of the solution measured in a cuvette:

$$\sqrt{\frac{T_o}{T_a}} - 1 = \frac{1.15L_{\text{eff}}}{L}A. \tag{5}$$

B. Absorbance spectra

Using a white light source, we can measure the light coupled through the microsphere over a broad wavelength range. With a sapphire hemisphere and selective choice of optical fibers and coupling lens, transmission from 230 to 950 nm was detected. Transmission may extend further into the infrared, but we were limited by light source and detector. The change in transmission when dye is flowed past the microsphere can be used to determine an absorbance spectrum, as shown in Fig. 4. With LGB dye dissolved in *p*H 5 sodium citrate/citric acid buffer solution, the absorbance spectrum measured in a dual beam Cary 100 Bio UV-visible spectrophotometer (Varian, Inc., Palo Alto, CA) (dashed line) was very similar to that determined from the microsphere measurement (solid line). These spectra have been normalized to allow comparison of their shapes. Comparing the magnitude of the change in the transmitted light, the microsphere measurement had a pathlength of 0.57 cm.

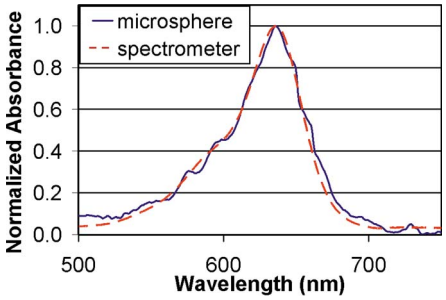

FIG. 4. (Color online) Absorbance spectra of LGB dye as measured using the microsphere system and a conventional spectrometer.

C. Flow cell absorbance measurements

Most measurements were carried out using LEDs as the light source. The transmission through the microsphere was monitored at the peak LED wavelength as a function of time as liquid was pumped through the microfluidic channel. Initially, water (or buffer solution) was pumped past the microsphere, allowing the measurement of the baseline transmission. Analyte solution was injected into a sample loop and then valves were switched to direct water through the sample loop, forcing the analyte solution past the microsphere. When some of the WGM light was absorbed by the analyte, the transmission decreased. As the analyte was pumped past the microsphere and again replaced by water, the transmission should return to the baseline. Further valve switches and injections were used for additional measurements.

Figure 5 shows a typical transmission signal, in this case for injections of LGB dye in *p*H 5 citrate buffer alternated with injections of isopropyl alcohol (IPA). The microsphere was excited using a 635 nm LED and the transmission was monitored at that wavelength. The IPA was used to assist in removing dye adsorbed to the microsphere surface between injections and to provide a repeatable reference signal in the data stream. The transmission drops during the IPA injection because of the change in refractive index, which affects the coupling to the microsphere. Injections of 0.5 ml were made into a sample loop and the flow rate of the liquid through the system was 0.5 ml/min. Therefore, a signal duration of 60 s would be expected. The actual width of the peaks, as measured when the transmission was halfway between the baseline transmission and the transmission with the analyte, was 76–81 s. Also, it is noticeable that the recovery of the trans-

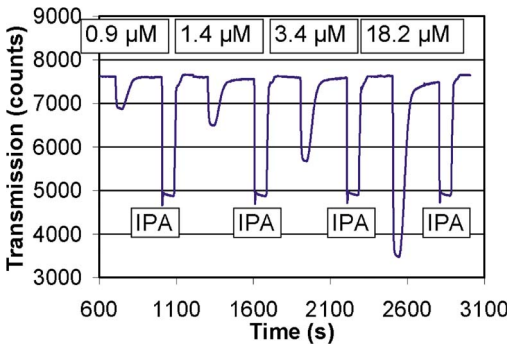

FIG. 5. (Color online) Transmission through the microsphere system as water (baseline of about 7600 counts), LGB dye (concentrations shown on the graph), or IPA travels past the vicinity of the microsphere.

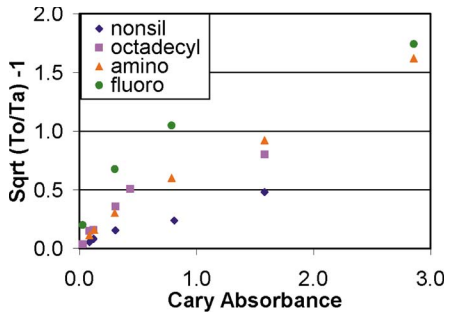

FIG. 6. (Color online) Relationship between absorbance measured in a conventional Cary spectrometer and with the microsphere system [according to Eq. (3)] for LGB dye at *p*H 5 and microspheres silanized with several coatings.

mission after the analyte occurs more slowly than the initial decrease. Mixing between the analyte and the water carrier due to the increased interaction time and amount of tubing through which they travel is a possible explanation. The kinetics of the decrease and recovery did not appear to be dependent on the dye or coating, suggesting that the kinetics are dominated by the flow rather than binding/unbinding of the dye to the coating.

As expected, the transmission decreased more if the LGB concentration was higher. Over this range of concentrations, we measured a linear relationship ($R^2 > 0.99$) between concentration and absorbance as measured by the Cary spectrophotometer. In Fig. 6, we show $\sqrt{T_o/T_a} - 1$ on the y axis versus the absorbance of the solution measured in a cuvette on the x axis. Results are given for the LGB dye in *p*H 5 citrate buffer with microspheres that have been treated with a variety of surface coatings. From Eq. (5), we expect a linear relationship with a slope equal to $1.15L_{\text{eff}}/L$. In all cases, there was more transmission at higher concentrations than would be expected, although this is more pronounced for the fluorosilanized and octadecylsilanized microspheres. Forcing a linear fit through the origin, effective pathlengths of 0.31, 0.58, 0.59, and 0.68 cm were determined for the nonsilanized, octadecylsilanized, aminosilanized, and fluorosilanized microspheres, respectively.

D. Effect of surface coatings

If the dye did not interact with the surface of the microsphere, the only effect the surface coating could have on the measured pathlength would be by absorbing some of the light or by increasing or decreasing scattering of the light at the microsphere surface. This would be a change in the losses of the resonator. If this is the case, all dyes measured at a given wavelength for a given surface coating would have the same effective pathlength.

Our studies were expanded to include the visible wavelength dyes SY, OG, and MB. Pathlengths were measured for each dye with microspheres of various coatings. The SY, OG, and MB dyes were dissolved in DI water. The LGB dye was dissolved in buffer solutions to hold the *p*H steady because the dye is very *p*H sensitive,[27] and we have observed a change in the absorbance spectrum due to the changing *p*H at different concentrations of the dye when dissolved in water. Measurements were made at *p*H 5 as discussed previously, but also at *p*H 7 and *p*H 9 using potassium phosphate/sodium hydroxide buffer. The SY and OG were measured using a 470 nm LED, while the LGB and MB were measured using a 635 nm LED.

Table I compares the pathlength (in centimeters) for each of the dyes measured with a nonsilanized microsphere. The expected net charge for each dye was calculated. It is clear from this chart that the pathlength for two dyes can be very different even when the dyes are measured at the same wavelength. This strongly suggests that the dyes interact with the surface of the microsphere. Generally, the transmission quickly returned to the baseline after a dye injection, so the surface interaction must be reversible and fast. Measurements were also carried out with microspheres having different surface coatings. The ratio of the pathlengths with different coatings compared to the nonsilanized microsphere is also shown in Table I.

The ODS coating was expected to make the surface of the microsphere hydrophobic. Because these dyes are all charged, we did not expect them to be attracted to the ODS coating; however, the LGB and, to a lesser extent, the MB were. The APTES coating was expected to be positively charged and the pathlength seemed to increase more for the more negatively charged dyes and decrease for the positively charged MB. The fluorosilane (PFDTES) coating was not expected to attract any of the dyes, but like the ODS coating, LGB and MB had a longer pathlength. The large increase in pathlength for LGB at *p*H 9 with the fluorosilane coating was such that the pathlength was similar for the LGB at all three *p*H values (~0.5 cm). We also observed that the SY had a pathlength about three times greater than that of the OG for the noncoated, aminosilane, and fluorosilane-coated microspheres even though the structure of these dyes is very similar.

The relatively large pathlengths observed with the ODS

TABLE I. Measured pathlengths for several dyes and changes in pathlength when the microsphere was silanized.

Dye	Charge	Pathlength for nonsilanized (cm)	Ratio of pathlength		
			ODS/nonsilanized	APTES/nonsilanized	PFDTES/nonsilanized
SY	−2	0.040	0.14	5.21	0.30
OG	−2	0.012	0.07	5.94	0.39
LGB *p*H 5	−1	0.23	4.55	2.37	2.59
LGB *p*H 7	−1.8	0.12		2.34	4.83
LGB *p*H 9	−2	0.03	4.92	5.44	15.73
MB	1	9.5	1.38	0.25	1.54

TABLE II. Expected effect of *p*H on the electrostatic charge of the aminosilane coating, benzylamine, and benzoic acid.

*p*H	Aminosilane	Benzylamine	Benzoic acid
3	Positively charged	Positively charged	More neutral
7	Positively charged	Positively charged	Negatively charged
10	More neutral	More neutral	Negatively charged

and fluorosilane-coated microspheres support the hypothesis that hydrophobic interactions between the dyes and the surface are occurring.

E. Benzylamine and benzoic acid

Because the dyes tested are not well characterized in the literature, we also investigated the response with simpler molecules. Benzoic acid and benyzlamine are water soluble, have very similar structure, and have absorbance in the 260 nm wavelength range. Benzylamine has a pK_a of 9.3 and should therefore be positively charged at *p*H 7. Benzoic acid has a pK_a of 4.2 and should be negatively charged at *p*H 7. The measured *p*H of an aqueous solution containing 0.3 mg/ml benzoic acid was 3.4, while the *p*H of a 1.5 μl/ml solution of benzylamine was 10.4. Half of each solution had the *p*H adjusted to ~7 by addition of either HCl or NaOH. The pK_a of the amine groups on the aminosilane surface coatings are not precisely known, as they are predicted to change when bound to a surface. However, the amine groups are expected to be positively charged at lower *p*H but more neutral at a *p*H near 10. Table II shows the expected charge for each group at the *p*H values used for testing.

We expected that the interactions between the aminosilane coatings and analytes would be weaker at *p*H 7 for benzylamine and stronger at *p*H 7 for benzoic acid. The measured pathlengths (in micrometers) are shown in Table III.

The results are as expected for benzylamine and the aminosilanes. However, for benzoic acid, even though the amine surface should be positively charged and the benzoic acid negatively charged at *p*H 7, there was less apparent interaction between it and two of the three aminosilanes. We thus suspect that hydrophobic attractions between the analytes and the surface play as large or larger a role than electrostatic forces in the interaction between the analytes and the surface. The APTES silane with its three reactive ethoxy groups was expected to result in a significantly greater density of amine groups on the microsphere surface than the APdMES silane, with only one reactive ethoxy group. Longer pathlengths (and therefore greater interaction with the microsphere) were measured for the benzoic acid, but the pathlengths were shorter for the benzylamine.

TABLE III. Pathlengths in micrometers determined for benzylamine and benzoic acid at different *p*H values with aminosilanized and nonsilanized microspheres.

	APTES	APdMES	APMdES	Nonsilanized
Benzylamine *p*H 7	99	131	98	74
Benzylamine *p*H 10	389	431	182	212
Benzoic acid *p*H 7	322	66	159	0
Benzoic acid *p*H 3	828	444	136	326

F. UV wavelength amino acids

We also tested the ability of our system to detect biomolecules. Amino acids are the building blocks for peptides and proteins and are more readily available. Three of the amino acids have absorbance peaks in the 250–300 nm wavelength range: tyrosine, tryptophan, and phenylalanine. In addition, tyrosine can undergo phosphorylation, a key step in signal transduction and regulation of enzymatic activity. Thus, one of the applications for microsphere detection that we considered was distinguishing between peptides and proteins with the ordinary amino acid L-tyrosine and phosphorylated L-tyrosine, called *o*-phospho-L-tyrosine. We prepared solutions at different concentrations due to differing solubility limits. In addition, phenylalanine and tryptophan have large molar extinction coefficients and more dilute solutions were required in order to be able to measure absorbance spectra on the Cary spectrometer.

Initial tests used an uncoated microsphere. Phenylalanine (1 mg/ml) was tested at 260 nm and found to have a pathlength of 74 μm with a standard deviation of 15%. Tryptophan was tested at 280 nm with both 0.1 and 1 mg/ml concentrations. The effective pathlengths were similar at 66 and 53 μm. Tyrosine was less soluble (0.35 mg/ml) and had a much lower measured absorbance on the Cary spectrometer. The decrease in transmission was just barely detectable with the microsphere system, but that still resulted in an effective pathlength of 225 μm.

o-phospho-L-tyrosine is more acidic than L-tyrosine. When both were dissolved in DI water at 0.3 mg/ml, the *p*H values of the solutions were 3.5 and 6.4, respectively. We also tested solutions of L-tyrosine (0.26 mg/ml) and *o*-phospho-L-tyrosine (0.18 mg/ml) in 10 mM MES acid buffer, which had *p*H values of 5.8 and 5.4, respectively. These are 1 mM solutions.

The UV-visible spectra are noticeably different. The L-tyrosine peak was at ~275 nm, while the *o*-phospho-L-tyrosine peak was at 265 nm. Absorbance measurements were made using a 260 nm LED (or 280 nm LED for the nonsilanized microsphere). Table IV shows the pathlengths measured with different coatings on the microspheres. In general, the amine-coated microspheres showed a greater pathlength for the *o*-phospho-L-tyrosine, indicating that the negatively charged molecule was interacting with the positively charged surface. The octadecyl-coated microsphere did not show a preference. The transmission data

TABLE IV. Pathlengths in micrometers for amino acids using microspheres with different silanization coatings.

Silanization of microsphere	L-tyrosine	*o*-phospho-L-tyrosine	L-tyrosine in MES buffer	*o*-phospho-L-tyrosine MES buffer
Nonsilanized (280 nm)	225			
APTES	182	874		
APMdES	126	415		
ODS	123	143	477	367

from the APTES-coated microsphere is shown in Fig. 7. Even though the L-tyrosine had a greater absorbance at 260 nm, the *o*-phospho-L-tyrosine injections resulted in a greater drop in the transmission. The transmission recovered somewhat after exposure to either molecule but did not completely recover until after injection of IPA.

G. Repeatability and detection limits

Although there was an effect from surface interactions which depended on both the microsphere surface coating and the analyte, the signal for a given microsphere and analyte was found to be very repeatable. Figure 8(a) shows a series of 40 injections alternating between 3.6 μM LGB dye in *p*H 5 buffer solution and IPA using a microsphere that had been coated with fluorosilane. Even though the transmission did not quite recover to the baseline after dye injection before IPA injection, the signal was very repeatable. Figure 8(b) compares the normalized transmission for three of the injections of dye. The first IPA/dye injections had a slightly different baseline, but even then, the decrease in transmission due to the dye was very similar to later injections. Comparing all 20 LGB injections, the pathlength of 0.42 cm had a standard deviation of 2.3%. A similar standard deviation in pathlength was measured for an aminosilane coating even though the baseline was gradually decreasing over those 20 injections.

In order to achieve a low detection limit and a large range of detectable absorbance values, not only is a large effective pathlength required but also a large baseline transmission through the microsphere system compared to the noise. Experiments with MB dye resulted in some of the largest pathlengths we measured and these data are used below to determine the detection limit for MB. Our solutions had absorbance of 0.085 and concentration of 1.4 μM. With the fluorosilane-coated microsphere and an integration time

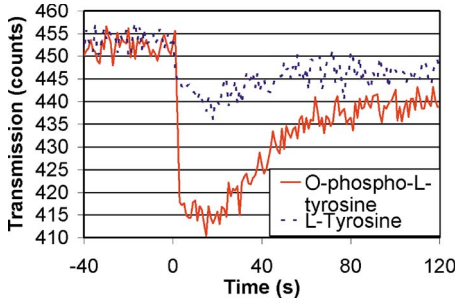

FIG. 7. (Color online) Transmission through the microsphere decreases when solutions of L-tyrosine or *o*-phospho-L-tyrosine flow past.

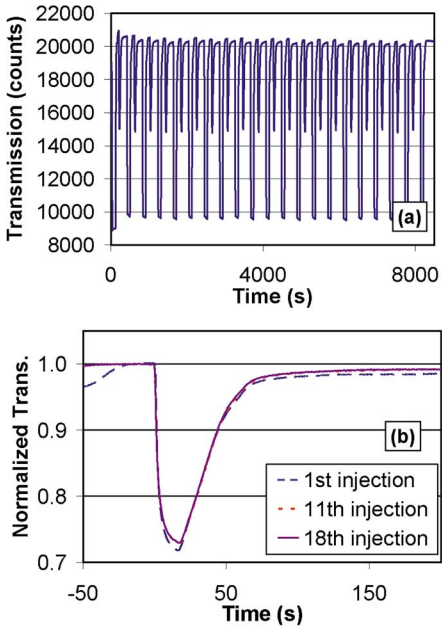

FIG. 8. (Color online) (a) Transmission through the microsphere system for 20 injections each of LGB dye and IPA. (b) Normalized comparison of the transmission for three of the injections of dye. The transmission of the 11th and 18th injections match so well as to be indistinguishable.

of 50 ms, the pathlength was 4.0 cm after the injection. There was a baseline of 25 000 counts. If we assume a transmission decrease of 20 counts (three times the standard deviation of the water baseline) as our minimum detectable signal, that transmission decrease corresponds to an absorbance of 0.087 mAU (milli-absorbance-unit)—about 1000 times smaller than the concentration we used. That value corresponds to about a 1.5 nM concentration (MB has a strong extinction coefficient of $\sim 6 \times 10^4$ mol^{-1} cm^{-1}). For an absorbance of 2 AU, there would still be at least 97 counts (an absorbance of 4 AU would have 24 counts). Using an integration time of 90 ms, which still allows a 10 Hz sampling rate, there would be more counts but similar noise, and the minimum detectable absorbance would be 0.05 mAU.

For comparison, the second-best data were obtained using an ODS coating. The pathlength was 6.7 cm with an integration time of 300 ms and a baseline of 8000 counts. This corresponds to a minimum absorbance of 0.16 mAU.

IV. DISCUSSION

We have demonstrated that broadband optical absorbance measurements can be made using a microsphere resonator in a microfluidic channel. The spectrometer covers both UV and visible wavelengths. Transmission through the system is high enough to allow the use of LEDs as the light source.

The molecules in the microfluidic channel interact with the microsphere surface, resulting in variations in the measured pathlength. The interaction of the analytes with the microsphere surface is undesirable for an absorbance spectrometer. However, such interactions are routinely taken advantage of by biosensors that detect biomolecule binding.[17] If the surface of the microspheres can be modified to interact

only with specific analytes (such as matching DNA strands or antibody-antigen pairs), this creates potential applications in the biological applications of micro-electro-mechanical-systems (BioMEMS) arena. This area, which embraces biochips and microfluidics, has an impact in gene sequencing, functional genomics, drug discovery, pharmocogenomics, diagnostics, and pathogen detection applications.

ACKNOWLEDGMENTS

Sai Chu, Oliver King, F. G. Johnson, and David Gill of the PLC Division of Infinera are thanked for their work in microfluidic chip fabrication. Tom Rendon and Dean Feken of ICx Nomadics carried out much of the engineering to integrate the fluidic setup. Joongho Moon, Dongyuan Piao, and Paul MacLean of ICx Nomadics provided suggestions for the testing of biomolecules. Software for data acquisition and fluidic controls was written by Philip Vickery of ICx Nomadics. This work was supported by NIST Advanced Technology Program Cooperative Agreement No. 70NANB4H3026.

[1] M. J. K. Thomas, *Ultraviolet and Visible Spectroscopy*, 2nd ed. (Wiley, Chichester, NY, 1996).
[2] L. R. Snyder, J. J. Kirkland, and J. L. Glajch, *Practical HPLC Method Development*, 2nd ed. (Wiley, Hoboken, NJ, 1997).
[3] N.-T. Nguyen and S. T. Werely, *Fundamentals and Applications of Microfluidics*, 2nd ed. (Artech House, Boston, 2006).
[4] J. Berthier and P. Silberzan, *Microfluidics for Biotechnology* (Artech House, Boston, 2006).
[5] M. L. Gorodetsky, A. A. Savchenkov, and V. S. Ilchenko, Opt. Lett. **21**, 453 (1996).
[6] T. M. Benson, S. V. Boriskina, P. Sewell, A. Vukovic, S. C. Greedy, and A. I. Nosich, *Frontiers in Planar Lightwave Circuit Technology*, NATO Science Series II: Mathematics, Physics and Chemistry, edited by S. Janz, J. Ctyroky, and S. Tanev (Sprinter, Dordrecht, The Netherlands, 2006).
[7] A. B. Matsko and V. S. Ilchenko, IEEE J. Sel. Top. Quantum Electron. **12**, 3 (2006).
[8] K. J. Vahala, Nature (London) **424**, 839 (2003).
[9] I. M. White, H. Oveys, and X. Fan, Opt. Lett. **31**, 1319 (2006).
[10] J. C. Knight, G. Cheung, F. Jacques, and T. A. Birks, Opt. Lett. **22**, 1129 (1997).
[11] M. Cai and K. Vahala, Opt. Lett. **25**, 260 (2000).
[12] M. Hossein-Zadeh and K. J. Vahala, Opt. Express **14**, 10800 (2006).
[13] A. Yariv, Electron. Lett. **36**, 321 (2000).
[14] M. L. Gorodetsky and V. S. Ilchenko, J. Opt. Soc. Am. B **16**, 147 (1999).
[15] S. Blair and Y. Chen, Appl. Opt. **40**, 570 (2001).
[16] K. A. Fuller and D. D. Smith, Opt. Express **15**, 3575 (2007).
[17] A. A. Savchenkov, A. B. Matsko, V. S. Ilchenko, and L. Maleki, Opt. Express **15**, 6768 (2007).
[18] V. S. Ilchenko and A. B. Matsko, IEEE J. Sel. Top. Quantum Electron. **12**, 15 (2006).
[19] E. Krioukov, D. J. W. Klunder, A. Driessen, J. Greve, and C. Otto, Opt. Lett. **27**, 512 (2002).
[20] K. De Vos, I. Bartolozzi, E. Schacht, P. Bienstman, and R. Baets, Opt. Express **15**, 7610 (2007).
[21] M. L. Gorodetsky and V. S. Ilchenko, Opt. Commun. **113**, 133 (1994).
[22] J. Zhang, B. N. Strecker, R. K. Shelton, S.-J. Ja, A. T. Rosenberger, and J. V. Hryniewicz, "A broadband whispering-gallery mode microsphere absorbance spectrometer," (submitted).
[23] J. H. Moon, J. H. Kim, K.-J. Kim, T.-H. Kang, B. Kim, C.-H. Kim, J. H. Hahn, and J. W. Park, Langmuir **13**, 4305 (1997).
[24] R. K. Iler, *The Chemistry of Silica: Solubility, Polymerization, Colloid and Surface Properties, and Biochemistry* (Wiley, New York, 1979).
[25] Note that the factor of 2.3 is often included in definitions of ε used by chemists but is not included by optical engineers.
[26] A. T. Rosenberger, Opt. Express **15**, 12959 (2007).
[27] D. M. Davies and A. U. Moozyckine, J. Chem. Soc., Perkin Trans. 1 **2**, 1495 (2000).